Ann. Geophys., 24, 1861–1869, 2006
www.ann-geophys.net/24/1861/2006/

Annales Geophysicae

Gadanki radar observations of daytime E region echoes and structures extending down to 87 km

A. K. Patra[1], **S. Sripathi**[2], **P. B. Rao**[3], **and R. K. Choudhary**[4]

[1]National Atmospheric Research Laboratory, Tirupati, India
[2]Indian Institute of Geomagnetism, New Panvel, Navi Mumbai, India
[3]National Remote Sensing Agency, Balanagar, Hyderabad, India
[4]Institute of Space and Atmospheric Studies, University of Saskatchewan, Saskatoon, Canada

Received: 6 February 2006 – Revised: 25 May 2006 – Accepted: 8 June 2006 – Published: 9 August 2006

Abstract. Observations of daytime E region echoes extending to altitudes as low as 87 km made using the Gadanki MST radar are presented. The echoing regions display descending layer resembling the characteristics of tidal winds and show structures with periods 2-4 min having both positive and negative slopes. At the center of the layer where strongest SNR is observed, the velocity is maximum and spectral width is minimum. At altitudes slightly above and below, where SNR is relatively low, velocity is low but spectral width is maximum. Daytime observations of echoes extending to such a low altitude and associated structures akin to nighttime quasi-periodic echoes throughout the observational period are the most significant results, not reported earlier from Gadanki and other locations. Other notable results are large SNR (as high as 15 dB) and spectral width (as high as 70 m/s) at the bottommost altitudes, where collisional damping of the plasma waves is significant.

Keywords. Ionosphere (Equatorial ionosphere; Ionospheric irregularities; Plasma waves and instabilities) – Meteorology and atmospheric dynamics (Turbulence)

1 Introduction

In the last one and half decade, there have been remarkable efforts to characterize and understand the generation mechanisms of mid- and low-latitude E region electron density irregularities and structures. Much attention has been paid to understand the genesis of quasi-periodic (QP) echoes, which were discovered by Yamamoto et al. (1991) using MU radar at Shigaraki, Japan. Initially thought to be an exclusive mid-latitude phenomenon, these echoes, although not as frequent, have now been detected from the low latitude stations like Gadanki (13.5° N, 79.2° E, 6.4° N Geomagnetic Latitude) in India (Choudhary and Mahajan, 1999; Choudhary et al., 2005) and Piura (5.2° S, 80.63° W, 7° N Geomagnetic Latitude) in Peru (Chau and Woodman, 1999) as well. They usually occur above 100 km during the night and have periods in the range of 2–20 min.

Another interesting aspect that has caught the researchers' attention are the plasma irregularity structures coming from the altitude below 100 km which have periods in the range of a few tens of seconds to 3 min (Urbina et al., 2000; Rao et al., 2000; Patra et al., 2002; Pan and Rao, 2002; Sripathi et al., 2003). Due to their occurrence at lower altitudes, they are also referred to as low-altitude-QP (LQP) echoes to differentiate them from the well-known QP echoes occurring at higher altitudes. While LQP echoes are known to occur both at low- and mid-latitudes, their occurrence during daytime have been reported only from low-latitude over Gadanki (Pan and Rao, 2002; Sripathi et al., 2003).

In this paper, we revisit the daytime plasma irregularity structures coming from lower E region using an experiment conducted with the Gadanki radar at a very high range resolution (∼150 m). Observations show a descending echo layer, which is about 3–4 km thick in altitude and has quasi-periodic structures embedded in it. A descending echo layer having a thickness of ∼3 km in altitude and extending down to height region as low as 88 km over Gadanki has already been reported by Choudhary et al. (1996). However, since the observations were taken for 10 min every half an hour with a range resolution of 600 m, there was not enough temporal and spatial information to go beyond the mere discovery stage. Later on, Sripathi et al. (2003) showed the structures associated with the descending daytime echo layer, but since those were detected only for a limited time interval above 93 km, many details of these irregularity structures could not get revealed. In the present communication, we present the observations, which show the occurrence of field aligned irregularity echoes almost continuously during the entire observation period of about 7.5 h. Of special interest is the

Correspondence to: A. K. Patra
(akpatra@narl.gov.in)

Published by Copernicus GmbH on behalf of the European Geosciences Union.

Table 1. Radar specifications and important parameters used for the E region field-aligned irregularities experiment.

Parameter	Value
Location	Gadanki (13.5° N, 79.2° E, 6.4° dip)
Frequency	53 MHz
Transmitted peak power	2.5 MW
Antenna gain	36 dB
Beam Width	3°
Beam Direction	13° N off-zenith
IPP	2000 μs
Coherent Integrations	4
FFT points	128
Incoherent Integrations	10
Range Resolution	150 m
Time Resolution	26 s
Height Range	85–140 km
Nyquist Velocity	175 m/s
Velocity Resolution	2.76 m/s

generation of plasma irregularities itself, which produce such coherent echo layer and the quasi-periodic structures embedded there in from the height range where collisional damping of the plasma waves is believed to be significant. We believe that the present observations provide a number of important information as far as the daytime low altitude E region FAI and associated structures are concerned.

2 Observations

The low altitude radar echoes reported here were made using the 53 MHz MST radar (Rao et al., 1995) located at Gadanki (79.2° E, 13.5° N, 6.3° N dip latitude). The experimental parameters used for the observations are given in Table 1. The experiment was conducted at a high range resolution of 150 m. Since for the E-region experiments, the radar beam is generally pointed 13° away from vertical and our two-way beam width is about 2° , the ambiguity in converting range to an actual altitude is of the order of only 550 m (Patra et al., 2002). In other words, a displacement in horizontal position as opposed to altitude could introduce a 550 m uncertainty in the determination of the altitude. This includes the uncertainty introduced by the refraction of the incident wave.

Figure 1 shows height time intensity (HTI) map of a low altitude echoes observed at Gadanki from the height range between 87 km and 98 km during 12:12 to 19:48 LT on 3 September 1997. The blank spaces in the HTI map represent the period when the radar was shutdown due to technical reasons. Height represents the vertical distance above the radar site, which is located about 400 m above the mean-sea-level. In this event, a ∼3 km thick echoing region descends from 98 km to 87 km with an average descent rate of ∼0.3 m/s. While descending, the echoing region also undergoes sinusoidal height variation. We will see later that inside the echo layer, there are some remarkable structures in terms of the variation of signal-to-noise ratio (SNR) with respect to time and height throughout the observational period of ∼7.5 h. The periods of the structures, however, vary as a function of height and time.

It is interesting to note in Fig. 1 that field aligned irregularities appear from the altitudes as low as 87 km. However, before we proceed for a detailed presentation of our result on the structures that we see inside the echo layer, we would like to summarize the spectral information of the entire dataset and their field alignment in order to compare them with what is commonly observed from neutral turbulence associated mesospheric echoes. This is in view of not to have any confusion on these echoes as high altitude mesospheric echoes. The spectral parameters (SNR, mean Doppler velocity and spectral width) are plotted in the form of histogram in Figs. 2a–c. SNR is found to be as high as 15 dB at 87 km and 30 dB at higher altitudes (0 dB detectability level is about –5 dB in this case) leading to a dynamic range of the echoes as high as 35 dB. The Doppler velocities are towards the radar (negative) and are less than 30 m/s. Spectral widths (2σ, where σ is the square root of the velocity variance) are in the range 10–100 m/s with higher values corresponding to higher altitudes. Notably, spectral width is found to be as high as 70 m/s at 87 km. Although no simultaneous observations with other beams were made on this day, experiments conducted at other times have clearly shown that such strong echoes are observed only from the direction that satisfies the perpendicularity with the magnetic field. While the field aligned property is valid for these echoes, we have not yet measured the exact aspect angle of these low altitude echoes.

Coming back to our Fig. 1, wherein we mentioned to see some fine structures embedded inside the echo layer, we may notice that the power associated with the echo structures appear to maximize in the middle of descending layer. In order to see the structures more clearly, we present two segments of data in Figs. 3 and 4 corresponding to the echoes coming from the higher and lower altitudes, respectively. In Figs. 3a–c, we present height-time maps of the three parameters, namely the SNR, mean velocity and spectral width corresponding to the observation seen between 93 km and 98 km, during 12:12 to 13:17 LT. In Figs. 4a–c, similarly, we show the height-time variations of same parameters but for height region 87 to 92 km observed during the time period between 18:54 LT and 19:48 LT. As mentioned before, SNR maps show that the power of echoes maximizes at the center of echo layer and decreases as we go above and below of the center maximum. Corresponding to the power maxima, it is interesting to note that while the Doppler velocity is also maximum at the center, the Doppler width is minimum and tends to maximize at the top and bottom of the layer. Obviously, therefore, the strongest SNR are associated with the

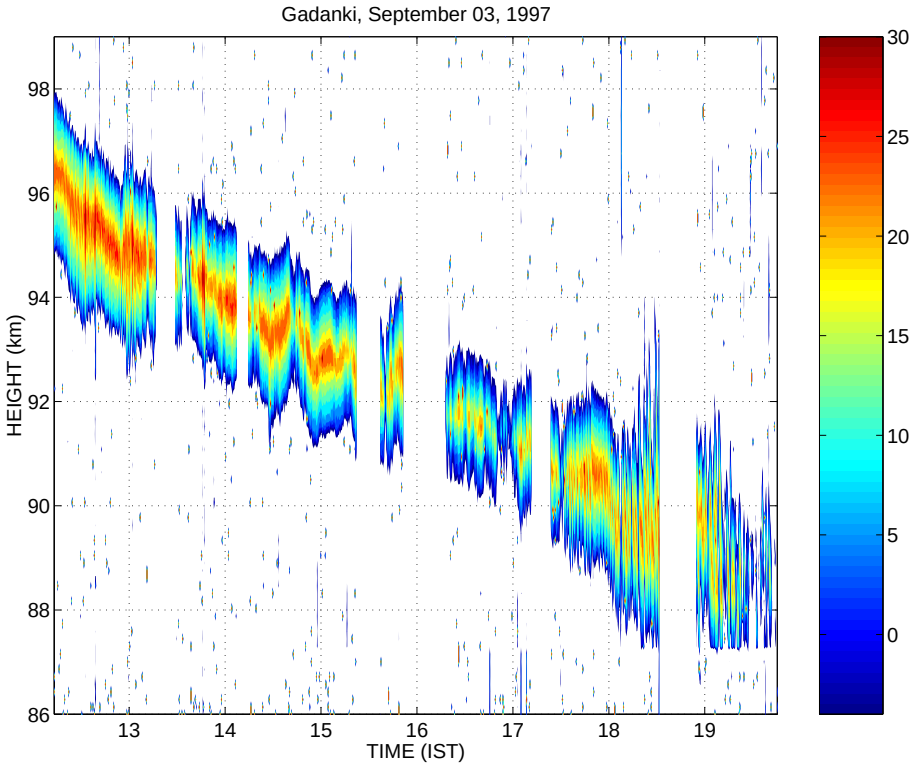

Fig. 1. Height-time-intensity (SNR) map of backscattered signals from E region observed on 3 September 1997. The blank spaces in the HTI map represent data gaps.

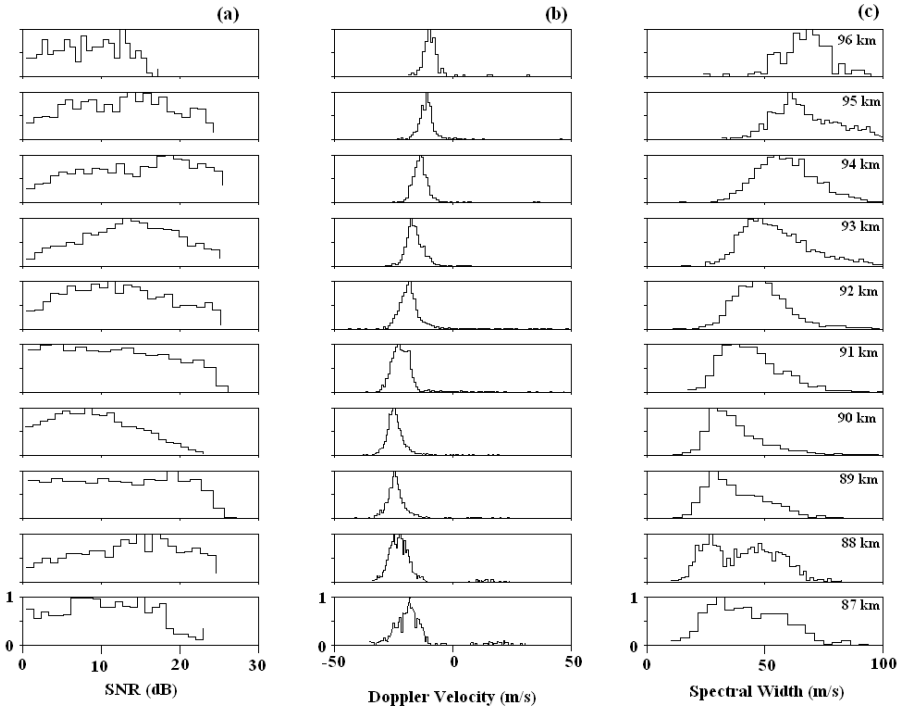

Fig. 2. Histograms of **(a)** SNR, **(b)** Velocity, and **(c)** Spectral width associated with the low-altitude echoes.

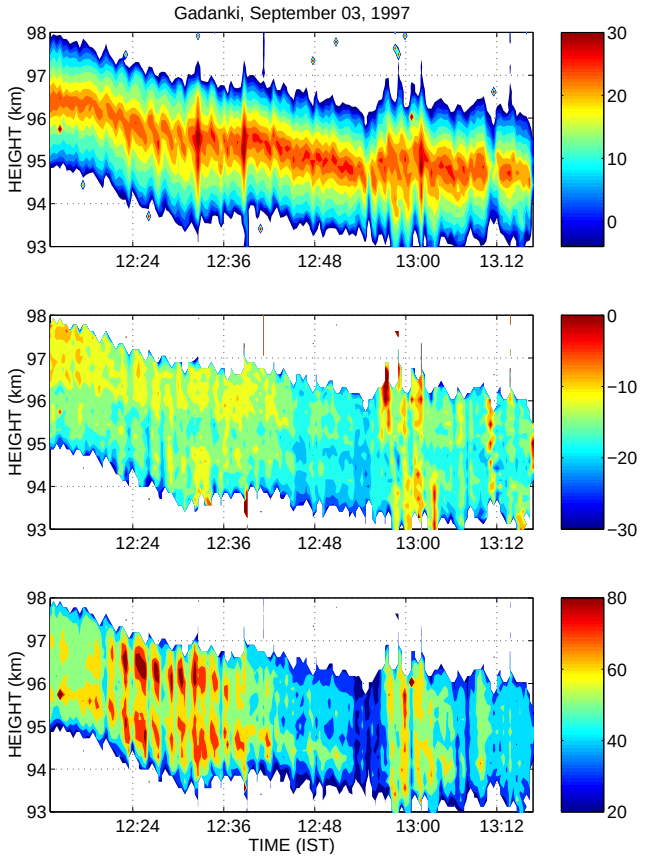

Fig. 3. Height-time variations of **(a)** SNR, **(b)** velocity, and **(c)** spectral width for the time period 12:12–13:17 LT.

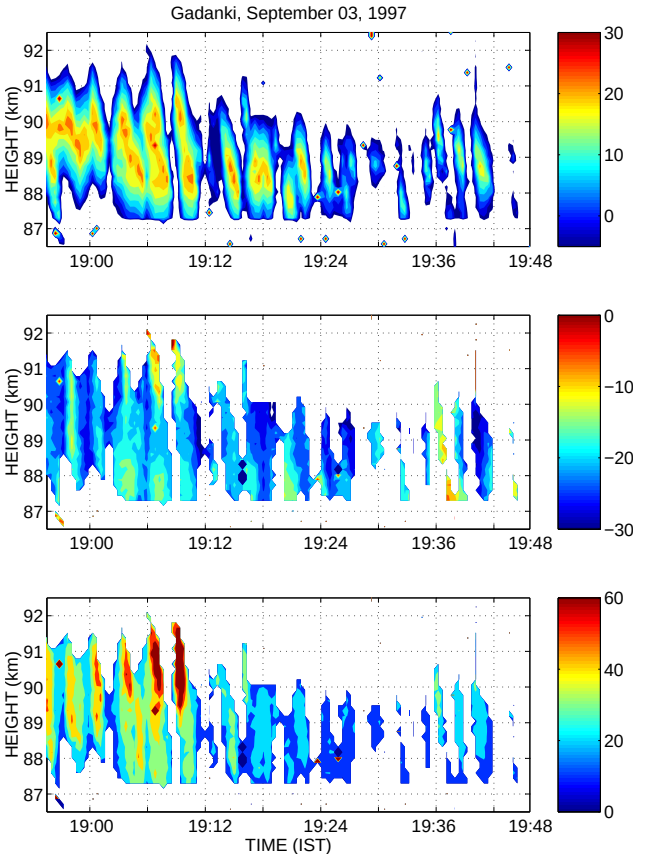

Fig. 4. Same as Fig. 3, but for period 18:54–19:48 LT.

larger Doppler velocity and small spectral width at the center of the layer while at the edges of layer, the SNR is low coupled with smaller velocity and larger spectral width. This observation is quite in contrast with what has been presented for the quasi-periodic striations associated with the echoes coming for height region above 100 km during night-time (Choudhary et al., 2005) wherein the power maxima at the center of echo layer always gets associated with a shear maxima (minimum Doppler velocity) and an enhanced Doppler width. We will discuss this aspect further in Sect. 3.2.

Altitude variation of SNR with respect to time shown in Figs. 3a and 4a further shows some remarkable structures inside the echo layer. While separated striations are clearly visible in SNR map of Fig. 4a, similar structures can also be discerned in Fig. 3a where the quasi-periodic structures gets reflected only in temporal and spatial variation of the signal intensity. Interestingly, distinct striated structures are more visible in the Doppler velocity and width maps than in the SNR maps, which are quite in contrast with the general understanding about QP echoes, which always seem to get associated with the intensity variation. It is worth mentioning here that a similar feature has been noted in the rest of the data set.

An eyeball estimation of the periodicity in the occurrence of striations inside the descending echo layer shown in Figs. 3 and 4 would suggest it to be of the order of 2 min. However, to accurately estimate the dominant periodicity of the structures, a spectral analysis using maximum entropy method along the line suggested by Barrodale and Erickson (1980) has been employed on the time series of SNR shown in Figs. 3a and 4a. The results are shown in Figs. 5a and 5b. Although the appearance of the echo structures in the SNR maps is so different, the dominant periods are quite similar and lie in the range of 2–4 min. The lower periods, however, are found to dominate in the first segment of the data shown in Fig. 3. Noteworthy is the periods, which are less than the Brunt Vaisala period (∼5 min at this height region). Structures with quite similar periodicity have been observed in the other segments of the data as well. To show that indeed the observations have similar structures, we present the time-height variation in the intensity of the rest of the data in Figs. 6a–d. Important point to note in these figures is the existence of both the positive and negative slopes in the structures, sometimes resembling to a saw-tooth shape.

To gain further insight into the observations, we examined the velocity data assuming that the mean Doppler velocities are due to meridional neutral wind (Krishna Murthy

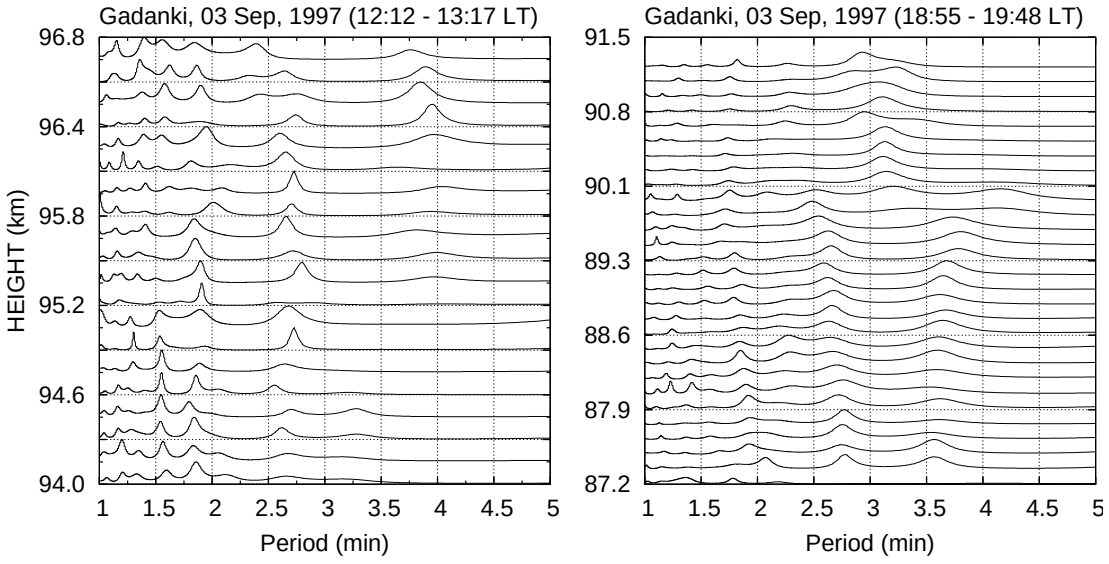

Fig. 5. Spectral density of dominant periods obtained through MEM for the observational period **(a)** 12:12–13:17 LT, and **(b)** 18:54–19:48 LT

et al., 1998). Meridional winds are estimated and found to be as high as 135 m/s southward corresponding to line-of-sight Doppler velocity of –30 m/s. Similar magnitude winds have been observed using rocket experiments (Larsen and Odom, 1997; Larsen et al., 1998) and hence are quite realistic. We then calculate the wind shears, which are shown in Fig. 7. These represent wind shear averaged over 15 min to smooth out the noise-like fluctuations. The shear values are mostly within ±20 m/s/km and occasionally exceeding this limit.

3 Discussion

From the observations presented above, we can summarize the main results as: (1) the daytime field-aligned echoes display descending echoing region resembling the tidal ion layer, (2) they occur at altitudes as low as 87 km and have remarkably large SNR and spectral width, (3) SNR variations show structures with periods 2–4 min, and (4) strongest SNR are associated with the larger Doppler velocity and small spectral width at the center of the layer as against the smaller SNR which are associated with smaller velocity and larger spectral width close to the edges of the layer.

Echoing layers having thickness of 2–3 km and descent rate of ∼0.5 m/s have already been reported from Gadanki observations (Choudhary et al., 1996; Patra et al., 2004; Pan and Rao, 2004). However, such echoes during daytime have been observed at Gadanki only. Descending E region echoing structures have been observed also at Piura in Peru (Woodman et al., 1999), a low-latitude station quite similar to Gadanki. A statistical study on the occurrence of coherent echoes from E region at Piura, reported by Chau et al. (2002), however clearly show that echoes, although occur down to ∼90 km, they are seen mostly at night between 19:00 LT and 07:00 LT. Such type of echoes has also been observed at Chung-Li (Pan and Tsunoda, 1998) and Arecibo (Urbina et al., 2000, 2004) as well, but again they have been seen only at night. In the light of above discussion, the irregularity structures observed during daytime at Gadanki assume special significance. Keeping in mind that all the features presented above are of vital importance to gain insight into the processes involved, we discuss them below in details.

3.1 Descending echoing layer and relevance of tidal ion layer

One important aspect of the present observations is the descending layer characteristics associated with these echoes observed in our data and also observed at other low-/mid-latitudes. They are reminiscence of tidal ion layers (Mathews, 1998) and suggest the possible role of tidal wind fields for manifesting the descending features. Another important and interesting aspect of the descending echoing region is the occurrence of echoes at altitudes as low as 87 km. Dynamics of E region layers in the height region of 80–160 km has been extensively studied both experimentally and theoretically over Arecibo (Mathews and Bekeny, 1979; Tong et al., 1988) and more recently using ionosonde at Milos (Haldoupis et al., 2006). Arecibo observations showed that the layer could come down to altitude as low as 85 km. It has been shown that below 100 km the layer dynamics is controlled by diurnal tide wherein the diurnal tide drags the layer down to altitude as low as 85 km (Mathews and Bekeny, 1979; Tong et al., 1988; Haldoupis et al., 2006). The fact that the echoing layer descended to altitude of 87 km with an average descent rate of 0.3 m/s suggests that the descending characteristics is very much consistent with the action of diurnal tide. The average descent rate of 0.3 m/s correspond

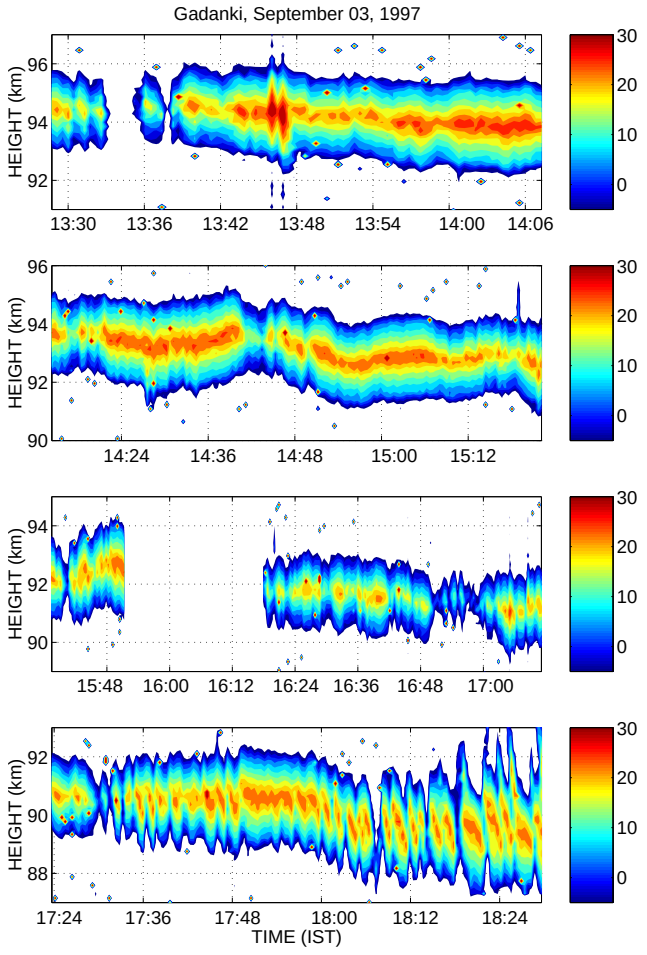

Fig. 6. Zoomed in version of height-time SNR maps for period **(a)** 13:28–14:07 LT, **(b)** 14:14–15:22 LT, **(c)** 16:37–17.12 LT, and **(d)** 17:23–18:31 LT.

to vertical tidal wavelength for the diurnal tide of about 26 km, which is very close indeed to the 25–30 km wavelength predicted by theory for the S(1,1) diurnal tide (Hagan and Forbes, 2002). Further, Urbina et al. (2000) have observed VHF radar echoes at altitudes as low as 90 km and have shown that they are associated with tidal ion layer observed simultaneously by the Arecibo incoherent scatter radar. Based on these facts, we infer that similar tidal ion layers must be responsible for the echo layer observed at Gadanki also.

3.2 Source of quasi-periodic structures

The structures have dominant periods of 2–4 min and have been observed throughout the observational period of ∼7.5 h. The fact that the growth of large-scale (kilometer scale) gradient drift waves (GDI) is not preferred in the height region of our interest (<97 km) (Pfaff, 1991; Wang and Bhattacharjee, 1994), the possibility of large-scale GDI as the causative mechanism for the observed features can be ruled out. Then when we turn to view these observations in terms of QP echoes, we have essentially three mechanisms: gravity wave related Es layer modulation and associated polarization process (Woodman et al., 1991; Tsunoda et al., 1994), wind shear driven Kelvin-Helmholtz (KH) instability (Larsen, 2000), and wind shear driven Es layer instability (Cosgrove and Tsunoda, 2002).

We will have to rule out the Cosgrove-Tsunoda (CT) mechanism out rightly at Gadanki because of its geometry. The Es layer in the CT theory has to be perpendicular to the magnetic field to start with. Since the magnetic field lines at Gadanki are almost horizontal the implication is that the distorted Es layer would start with a near vertical position. This is, in a way, very difficult to achieve from a simple horizontal starting point created by the usual zonal wind shear mechanism. Further, the echoing layer is located in the collision dominated lower E region, where it would be difficult to realize polarization field required for the instability to grow.

Choudhary et al. (2005) have made a detailed study on the QP echoes of periodicities less than Brunt Vaisala period (∼5 min) observed at altitudes above 100 km by the Gadanki radar. Based on their observed periodic upward and downward velocity patterns as a proxy of KH flow pattern, they suggested the KH instability as the most plausible candidate responsible for their observations. Choudhary et al. (2005), however, based their discussion for KH billows on the following three facts: (1) Power maximum at the center of billows, (2) Enhanced Doppler width at the power maximum, and (3) the shear maximum at the power maximum. However, if we compare these preambles with what we have in our observations, we see that these conditions are not satisfied. We have (1) Power maximizing at center – as with the KH case, (2) the shear is minimum at the power maximum – opposite to the KH thesis, and (3) Doppler width maximizes at the top and bottom of layers where the shear is maximum - another point, which does not agree with KH hypothesis.

For the KH instability to set in, the Richardson number R_i should be <0.25, where $R_i = N^2/(dv/dz)^2$, N is the Brunt Vaisala frequency and dv/dz is the vertical shear in the horizontal wind. Considering the Brunt Vaisala period to be 5 min for the height of our interest, the required wind shear for the growth of the instability comes out to be >40 m/s/km. But the shears in the meridional winds are found to be much less. The possibility, however, may lie with zonal wind shear but we have no evidence for that. Although in principle, zonal wind shear can form a layer as well as make it unstable when it satisfies the condition of KHI, it may not do both simultaneously and for such a long time. When we analyzed our velocity data like that done by Choudhary et al. (2005), we found that the velocity perturbations are in the range 5–10 m/s, which are much less than their values (20–50 m/s). These facts further indicate that the likelihood of KHI is also remote.

Coming to the gravity wave theory of Woodman et al. (1991), Choudhary et al. (2005) have argued that there is

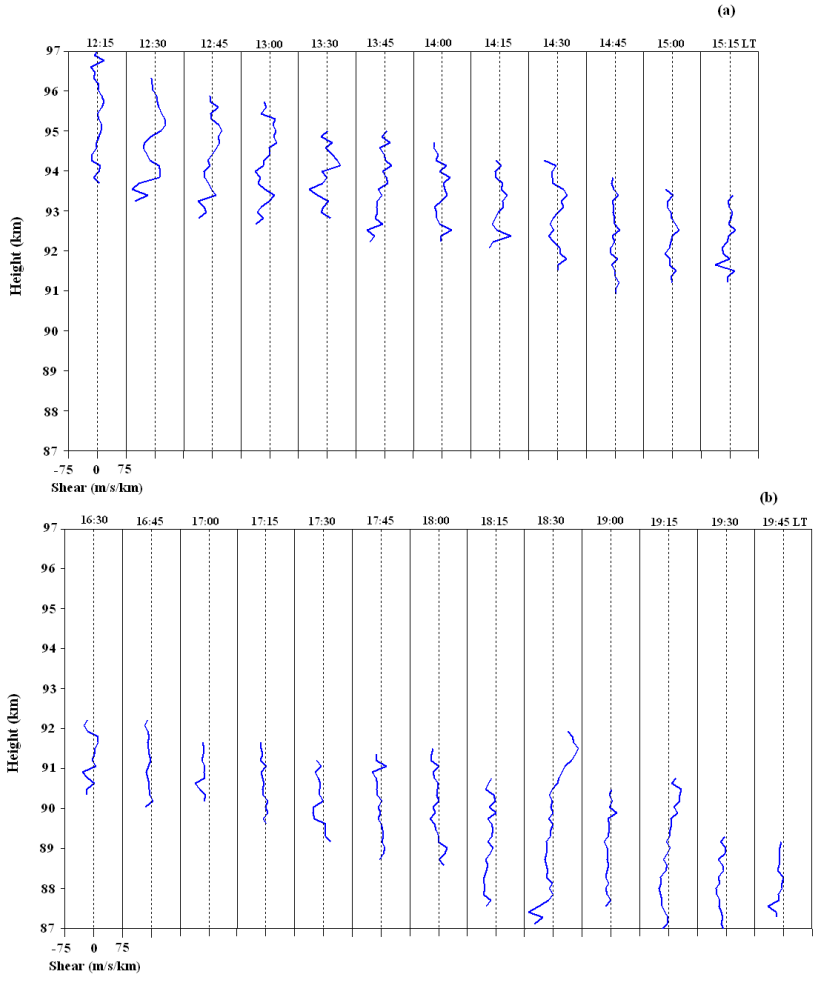

Fig. 7. Meridional wind shears computed from 15 min averaged velocity data.

a genuine difficulty to account for the short periods since very large winds are required to reduce the intrinsic period to the level of observed periodicity. While this may be logical to think for the gravity waves propagating in the magnetic meridian plane, we propose instead that zonally propagating short period acoustic gravity waves can be considered as a potential candidate for the observed features. In this case, the structures can be considered as enhanced density layers moving downward with the maximum shear zone associated with the upward propagating gravity waves. Urbina et al. (2004) have put forward quite similar mechanism to explain their observations. This, however, needs to be examined critically.

3.3 Generation of meter scale irregularities

As far as the low-altitude echoes are concerned, signal strength and spectral width are remarkably high as compared to their mesospheric counterpart. Further, the field-aligned properties of these irregularities suggest that these irregularities are not directly generated by neutral turbulence (Gurevich et al., 1997). Neutral turbulence, however, can have imprint on plasma at larger scale to excite plasma instability (Tsunoda et al., 1999).

The plasma instability process, that we know, relevant for the lower part of the E region is the gradient drift instability. But this instability also has limitation when we consider the collision dominated lower altitudes. For the radar geometry employed here, the 3-m waves are basically secondary waves. For the vertically propagating 3-m waves in the lower part of the equatorial electrojet, Kudeki et al. (1987) showed that the smallest possible threshold velocity required is 80–100 m/s when L values are 120–150 m. They have also argued that such scale lengths can be justified when the density gradients associated with intermediate-scale (50–100 m) waves are considered. Since the waves are observed with very small phase velocities, they suggested that the nonlinear mode coupling (Sudan and Keskinen, 1979) might be an efficient mechanism for transferring the energy from the large scale to small scale. In this sense, the characteristics of 3-m

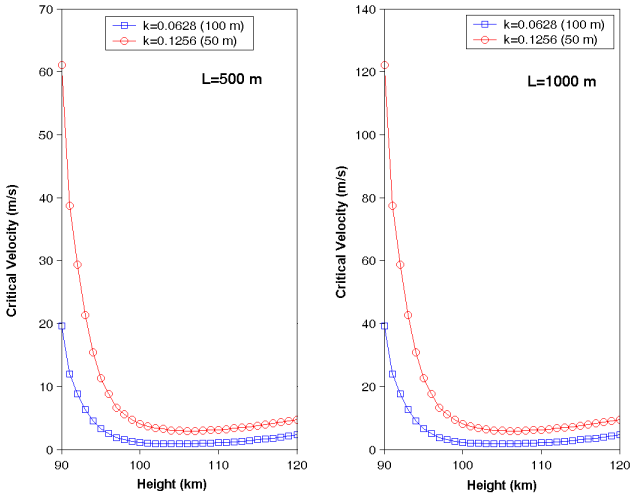

Fig. 8. Threshold velocity required for the growth of 50 m and 100 m gradient drift waves when L values are 500 m and 1000 m

irregularities at the lower E region reported here appears to be identical to the low altitude electrojet echoes (Kudeki et al., 1987).

For inclined magnetic field line geometry, it is important to consider the field line shorting effects while dealing with large-scale primary waves (Woodman et al., 1991). At the E region height over Gadanki, the dip angle is 13°. Corresponding to a layer of 1 km thickness (similar to that observed by Urbina et al. (2000), the length of the field line connecting the top and bottom of the layer is about 4.5 km. The electric potential mapping relation has been given as $\lambda_{\perp} \leq \lambda_{\parallel} / (\frac{\sigma_o}{\sigma_p})^{1/2}$ (Farley, 1960), where $\lambda_{\perp}$ and $\lambda_{\parallel}$ are the perturbation wavelengths perpendicular and parallel to the magnetic field, respectively and σ_o and σ_p are the parallel and perpendicular conductivity, respectively. For the height region of 90 and 100 km, $(\frac{\sigma_o}{\sigma_p})^{1/2}$ is 50 and 70, respectively. Accordingly, for a 1 km thick electron density layer, the corresponding longest waves that will grow are 90 m and 65 m. Since waves with larger wavelength will be damped, structures with wavelengths more than these, in principle, are not expected through gradient drift instability. This has important implication, since shorter the wavelength, larger is the threshold velocity required for their growth.

To elucidate the problem, we calculated the threshold velocity required for the growth of 50 and 100 m using vertical L value of 500 and 1000 m. L represents the vertical electron density gradient scale length. The results are shown in Fig. 8. It may be noted that the required drift velocity increases rapidly with decreasing height. At 90 km, for L of 500 m and 1000 m, the lowest value of drift velocity required for 50 m wave to grow are 60 m/s and 120 m/s, respectively. These values become 20 m/s and 40 m/s for 100 m wave. The above analysis suggests that the threshold values required are quite realistic. Once these intermediate scale waves grow, the 3-m scale waves responsible for the radar observations may grow subsequently through mode coupling as suggested by Kudeki et al. (1987).

While the intermediate scale waves are assumed to be instrumental for the generation of meter-scale irregularities, the quasi-periodic structure and the descending echoing layer suggest the potential role of neutral dynamics. In this context, the rocket borne observations of the lower E region irregularities made by Prakash et al. (1969) appears to be relevant, which have shown superposition of two different spectra: one due to neutral turbulence and the other due to electric fields.

4 Concluding remarks

We have presented observations of field-aligned E region irregularities and structures in a daytime descending echoing region from 98–87 km. The descent rate agrees with the descending phase speed of diurnal tide. The structures having periods of the order of 2–4 min throughout the observational period is most remarkable result among other results viz., large SNR and spectral width at the bottommost height. Although the generation mechanism of these structures is not singled out, we propose that zonally propagating short period acoustic gravity waves may be potential candidate.

Acknowledgements. The authors are grateful to the NARL technical staff whose dedicated efforts made possible the observations reported here. We acknowledge a very useful discussion with J. P. St-Maurice. The work of R. K. Choudhary has been supported by Canadian National Science and Engineering Research Council. Helpful suggestions from the referees of this paper are gratefully acknowledged.

Topical Editor M. Pinnock thanks two referees for their help in evaluating this paper.

References

Barrodale, I. and Erickson, R. E.: Alogrithm for least-square linear prediction and maximum entropy spectral analysis-Part I: Theory, Geophysics, 45, 420–432, 1980.

Chau, J. L. and Woodman, R. F.: Low-latitude quasiperiodic echoes observed with Piura VHF radar in E-region, Geophys. Res. Lett., 26, 2167–2170, 1999.

Chau, J. L., Woodman, R. F., and Flores, L. A.: Statistical characteristics of low latitude ionospheric field aligned irregularities obtained with the Piura VHF radar, Ann. Geophys., 20, 1203–1212, 2002.

Choudhary, R. K. and Mahajan, K. K.: Tropical E-region field aligned irregularities: Simultaneous observations of continuous and quasiperiodic echoes, J. Geophys. Res., 104, 2613–2619, 1999.

Choudhary, R. K., Mahajan, K. K., Singh, S., Kumar, K., and Anandan, V. K.: First VHF radar radar oservations of tropical latitude E-region field aligned irregularities, Geophys. Res. Lett., 23, 3683–3686, 1996.

Choudhary, R. K., St.-Maurice, J.-P., Kagan, L., and Mahajan, K. K.: Quasi-periodic backscatter from E region at Gadanki: evidence for Kelvin-Helmholtz billows in the lower thermosphere, J. Geophys. Res., 110, doi:10.1029/2004JA010987, 2005.

Cosgrove, R. and Tsunoda, R. T.: A direction-dependent instability of sporadic-E layers in the nighttime midlatitude ionosphere, Geophys. Res. Lett., 29(18), 1811, doi:10.1029/2002GL014669, 2002.

Farley, D. T.: A Theory of Electrostatic Fields in the Ionosphere at Nonpolar Geomagnetic Latitudes, J. Geophys. Res., 65, 869–877, 1960.

Gurevich, A. V., Borisov, N. V., and Zybin, K. P.: Ionospheric turbulence induced in the lower part of the E region by turbulence of the neutral atmosphere, J. Geophys. Res., 102, 379–388, 1997.

Hagan, M. E. and Forbes, J. M.: Migrating and nonmigrating diurnal tides in the middle and upper atmosphere excited by tropospheric latent heat release, J. Geophys. Res., 107, 4754, doi:10.1029/2001JD001236, 2002.

Haldoupis, C., Meek, C., Christakis, N., Pancheva, D., and Bourdillon, A.: Ionogram Height-Time-Intensity observations of descending sporadic E layers, J. Atmos. Solar-Terr. Phys., 68, 539–557, 2006.

Krishna Murthy, B. V., Ravindran, S., Viswanathan, K. S., Subbarao, K. S. V., Patra, A. K., and Rao, P. B.: Small-scale ($^-$3 m) E region irregularities at and off the magnetic equator, J. Geophys. Res., 103, 20 761–20 773, doi:10.1029/98JA00928, 1998.

Kudeki, E., Fejer, B. G., Farley, D. T., and Hanuise, C.: The Condor equatorial electrojet campaign – Radar results, J. Geophys. Res., 92, 13 561–13 577, 1987.

Larsen, M. F.: A shear instability seeding mechanism for quasiperiodic radar echoes, J. Geophys. Res., 105, 24 931–24 940, 2000.

Larsen, M. F. and Odom, O. D.: Observations of altitudinal and latitudinal E region neutral wind gradients near sunset at the magnetic equator, Geophys. Res. Lett., 24, 1711–1714, 1997.

Larsen, M. F., Fukao, S., Yamamoto, M., Tsunoda, R. T., Igarashi, K., and Yamamoto, M.: The SEEK chemical release experiment: Observed neutral wind profile in a region of sporadic E, Geophys. Res. Lett., 25, 1789–1792, 1998.

Mathews, J. D.: Sporadic E: Current views and recent progress, J. Atmos. Solar Terr. Phys., 58, 413–435, 1998.

Mathews, J. D. and Bekeny, F. S.: Upper atmospheric tides and vertical motion of ionospheric sporadic layers at Arecibo, J. Geophys. Res., 84, 2743–2750, 1979.

Pan, C. and Rao, P.: Morphological study of the field-aligned E-layer irregularities observed by the Gadanki VHF radar, Ann. Geophys., 22, 3799–3804, 2004.

Pan, C. J. and Rao, P. B.: Low altitude quasi-periodic radar echoes observed by the Gadanki VHF radar, Geophys. Res. Lett., 29, 3799–3804, 2002.

Pan, C. J. and Tsunoda, R. T.: Quasiperiodic echoes observed with the Chung-Li VHF radar during the SEEK campaign, Geophys. Res. Lett., 25, 1809–1812, 1998.

Patra, A. K., Sripathi, S., Sivakumar, V., , and Rao, P. B.: Evidence of kilometer-scale waves in the lower E region from high resolution VHF radar observations over Gadanki, Geophys. Res. Lett., 29, doi:10.1029/2001GL013340, 2002.

Patra, A. K., Sripathi, S., Sivakumar, V., and Rao, P. B.: Statistical characteristics of VHF radar observations of low latitude E region irregularities over Gadanki, J. Atmos. Solar-Terr. Phys., 66, 1615–1626, 2004.

Pfaff, R. F.: Rocket observations in the equatorial electrojet: Current status and critical problems, J. Atmosp. Terr. Phys., 53, 709–7288, 1991.

Prakash, S., Gupta, S. P., and Subbaraya, B. H.: Irregularities in the equatorial E region over Thumba, Radio Sci., 4, 791–796, 1969.

Rao, P. B., Jain, A. R., Kishore, P., Balamurlidhar, P., Damle, S. H., and Viswanathan, G.: Indian MST radar, 1. System description and sample wind measurements in ST mode, Radio Sci., 30, 1125–1138, 1995.

Rao, P. B., Yamamoto, M., Uchida, A., Hassenpflug, I., and Fukao, S.: MU radar observations of kilometer-scale waves in the midlatitude lower E-region, Geophys. Res. Lett., 27, 3667–3670, doi:10.1029/2000GL003820, 2000.

Sripathi, S., Patra, A. K., Sivakumar, V., and Rao, P. B.: Shear instability as a source of the daytime quasi-periodic radar echoes observed by the Gadanki VHF radar, Geophys. Res. Lett., 30, 2149, doi:10.1029/2003GL017544, 2003.

Sudan, R. N. and Keskinen, M. J.: Theory of strongly turbulent two-dimensional convection of low-pressure plasma, Phys. Fluids, 22, 2305–2314, 1979.

Tong, Y., Mathews, D, J., Ying, and W-P: An upper E region quarterdiurnal tide at Arecibo?, J. Geophys. Res., 93, 10 047–10 051, 1988.

Tsunoda, R. T., Fukao, S., and Yamamoto, M.: On the origin of quasiperiodic radar backscatter from midlatitude sporadic E, Radio Sci., 29, 349–366, 1994.

Tsunoda, R. T., Buonocore, J. J., Saito, A., Kishimoto, T., Fukao, S., and Yamamoto, M.: First observations of quasiperiodic echoes from Stanford, California, Geophys. Res. Lett., 26, 995–998, 1999.

Urbina, J., Kudeki, E., Franke, S. J., Gonzalez, S., Zhou, Q., and Collins, S. C.: 50 MHz radar observations of mid-latitude E-region irregularities at Camp Santiago, Puerto Rico, Geophys. Res. Lett., 27, 2853–2856, doi:10.1029/2000GL000028, 2000.

Urbina, J., Kudeki, E., Franke, S. J., and Zhou, Q.: Analysis of a mid-latitude E-region LQP event observed during the Coqui 2 Campaign, Geophys. Res. Lett., 31, L14 805, doi:10.1029/2004GL020031, 2004.

Wang, X.-H. and Bhattacharjee, A.: Gradient drift eigenmodes in the equatorial electrojet, J. Geophys. Res., 99, 13 219–13 226, 1994.

Woodman, R. F., Yamamoto, M., and Fukao, S.: Gravity wave modulation of gradient drift instabilities in midlatitude sporadic E irregularities, Geophys. Res. Lett., 18, 1197–1200, 1991.

Woodman, R. F., Chau, J. L., Aquino, F., Rodriguez, R. R., and Flores, L. A.: Low-latitude ionospheric field-aligned irregularities observed in the E-region with Piura VHF radar, Radio Sci., 34, 983–990, 1999.

Yamamoto, M., Fukao, S., Woodman, R., Ogawa, T., Tsuda, T., and Kato, S.: Midlatitude E-region field aligned irregularities observed with the MU radar, J. Geophys. Res., 96, 15 943–15 949, 1991.